Time-Varying Magnetic Field Produced by a Vibrating Aluminum Enclosure

Dr. John P. Casey
Submarine Electromagnetic Systems Department

Naval Undersea Warfare Center Detachment
New London, Connecticut

Report Documentation Page	*Form Approved* *OMB No. 0704-0188*

1. REPORT DATE **12 APR 1993**	2. REPORT TYPE **Technical Memo**	3. DATES COVERED **12-04-1993 to 12-04-1993**

4. TITLE AND SUBTITLE **Time-Varying Magnetic Field Produced by a Vibrating Aluminum Enclosure**	5a. CONTRACT NUMBER
	5b. GRANT NUMBER
	5c. PROGRAM ELEMENT NUMBER
6. AUTHOR(S) **John Casey**	5d. PROJECT NUMBER
	5e. TASK NUMBER
	5f. WORK UNIT NUMBER

7. PERFORMING ORGANIZATION NAME(S) AND ADDRESS(ES) **Naval Undersea Warfare Center Detachment,New London,CT,06320**	8. PERFORMING ORGANIZATION REPORT NUMBER **TM 931044**

9. SPONSORING/MONITORING AGENCY NAME(S) AND ADDRESS(ES) **Office of Naval Research**	10. SPONSOR/MONITOR'S ACRONYM(S) **ONR**
	11. SPONSOR/MONITOR'S REPORT NUMBER(S)

12. DISTRIBUTION/AVAILABILITY STATEMENT
Approved for public release; distribution unlimited

13. SUPPLEMENTARY NOTES
NUWC2015

14. ABSTRACT

Circuit theory is applied in the determination of the time-varying axial magnetic field produced by the interaction of a vibrating aluminum enclosure and the earth's magnetic field. The axial magnetic field that exists within the enclosure is received by a loop antenna. A steady-state time-harmonic analysis is applied. Theoretical results are compared with measured data at 100Hz.

15. SUBJECT TERMS
Circuit theory

16. SECURITY CLASSIFICATION OF:			17. LIMITATION OF ABSTRACT	18. NUMBER OF PAGES	19a. NAME OF RESPONSIBLE PERSON
a. REPORT **unclassified**	b. ABSTRACT **unclassified**	c. THIS PAGE **unclassified**	**Same as Report (SAR)**	**26**	

Standard Form 298 (Rev. 8-98)
Prescribed by ANSI Std Z39-18

ABSTRACT

Circuit theory is applied in the determination of the time-varying axial magnetic field produced by the interaction of a vibrating aluminum enclosure and the earth's magnetic field. The axial magnetic field that exists within the enclosure is received by a loop antenna. A steady-state time-harmonic analysis is applied. Theoretical results are compared with measured data at 100 Hz.

ADMINISTRATIVE INFORMATION

ACKNOWLEDGEMENTS

TABLE OF CONTENTS

LIST OF ILLUSTRATIONS

1. INTRODUCTION

Consider an aluminum enclosure of length L = 76 in. with a triangular cross section of width W = 33 in. and height H = 25 in. as shown in Fig. 1. The walls of the enclosure are 4 in. thick with the exception of the base which is 5 in. thick. The enclosure is sealed at both ends and provides sufficient shielding of atmospheric noise for frequencies of 50 - 100 Hz. Within the enclosure lies a loop antenna with a magnetic core. The loop antenna is in the form of a solenoid consisting of 30,800 turns of 26 gauge copper wire that are wound in 6 separate sections with 22 layers per section. The magnetic core is a circular cylinder of 4 ft length and 2 in. diameter.

The enclosure is made to vibrate while the loop antenna is held stationary within a vibration isolation system. The interaction of the moving enclosure with the earth's dc magnetic field is equivalent to a time-varying magnetic flux within the enclosure, inducing a current in the aluminum. The component of current flowing in the cross-sectional plane of the enclosure produces a time-varying axial magnetic field within the enclosure that is received by the loop antenna. The frequency of the measured magnetic field is correlated with the vibration frequency of the enclosure.

The purpose of this study is to determine the time-varying axial magnetic field received by the loop antenna due to the vibratory motion of the aluminum enclosure. A steady-state time-harmonic analysis will be applied.

2. ENCLOSURE MODEL

Fig. 2 illustrates three types of vibratory motion of the enclosure: (a) translational motion in the radial direction, (b) translational motion in the axial direction, and (c) rotational motion. The actual vibratory motion consists of a combination of these types of motion. The enclosure is made of aluminum, a good conductor ($\sigma = 3.77 \times 10^7$ S/m), and can be thought of as a fluid of free electrons. As the enclosure vibrates, the free electrons in the metal interact with the earth's dc magnetic field resulting in a Lorentz force experienced by each electron. The net effect of these forces is to produce an electric current in the aluminum. Because of the vibrating motion of the enclosure, this current will be time varying.

A current circulating in the cross-sectional plane of the enclosure is necessary to produce an axially directed magnetic field that can be received by the loop antenna. Therefore, the only motion of interest in this problem is one which results in a circumferentially directed current. To better understand which types of vibratory motion will produce a circumferential current in the aluminum, let us approximate the geometry of the enclosure by a tubular cylinder as in Fig. 2. For

the translational motions in Fig. 2 (a)-(b), diametrically opposite electrons in the cylinder will experience the same Lorentz force, resulting in a current distribution with no net circumferential flow regardless of the orientation of the earth's magnetic field. Consequently, translational motion is of no interest in this problem. In contrast, rotational motion of the enclosure results in a time-varying axial magnetic flux through the shield, producing an induced electromotive force (emf) in the enclosure. This induced emf produces a time-varying, circumferentially directed current distribution in the aluminum.

To determine the induced emf in the enclosure, consider the rotational vibration of the enclosure about its center in the x-z plane with coordinate system shown in Fig. 3, where the z axis is coincident with the axis of the enclosure. The primed coordinates refer to the rest frame of the enclosure while the unprimed coordinates refer to the earth's reference frame. The angle θ that the primed coordinate axes make with respect to the unprimed axes is given by

$$\theta(t) = \theta_o \sin \omega t \tag{1}$$

where $\omega = 2\pi f$ is the angular frequency of vibration and θ_o is the amplitude of vibration. Note that for vibrations of interest, $|\theta_o| \ll 1$.

The earth's dc magnetic field (flux density) is given in each reference frame as

$$\mathbf{B} = \mathbf{i}\, B_{xo} + \mathbf{j}\, B_{yo} + \mathbf{k}\, B_{zo} \tag{2a}$$

$$\mathbf{B}' = \mathbf{i}'\, B_x' + \mathbf{j}'\, B_y' + \mathbf{k}'\, B_z' \tag{2b}$$

where $\mathbf{i}$, $\mathbf{j}$, and $\mathbf{k}$ are the unit vectors along the x, y, and z axes, respectively, while $\mathbf{i}'$, $\mathbf{j}'$, and $\mathbf{k}'$ are the unit vectors along the x', y', and z' axes, respectively. Since the vibration is confined to the x-z plane, $\mathbf{j} = \mathbf{j}'$. The components of the earth's field in the enclosure frame are given in terms of the unprimed components as follows:

$$B_x' = B_{xo} \cos \theta + B_{zo} \sin \theta \tag{3a}$$

$$B_y' = B_{yo} \tag{3b}$$

$$B_z' = -B_{xo} \sin \theta + B_{zo} \cos \theta \tag{3c}$$

Note that the field components in the primed frame in eqs. (3) are time varying since θ is a function of time. The axial magnetic flux passing through the enclosure is

$$\Phi(t) = \iint B_z'\, dA = -B_{xo}\, A \sin \theta + B_{zo}\, A \cos \theta \tag{4}$$

where A is the cross-sectional area within the enclosure. It should be observed that the y component of the earth's magnetic field produces no contribution to the axial magnetic flux. The rate of change of flux through the enclosure is

$$\Phi'(t) = -B_{xo}A\omega\theta_o \cos\omega t \cos\theta(t) - B_{zo}A\omega\theta_o \cos\omega t \sin\theta(t)$$

$$\cong -B_{xo}A\omega\theta_o \cos\omega t - B_{zo}A\frac{\omega}{2}\theta_o^2 \sin2\omega t$$

$$= -\text{Re}\left\{V_1 e^{j\omega t} + V_2 e^{j2\omega t}\right\} \tag{5}$$

where

$$V_1 = B_{xo}A\omega\theta_o \tag{6a}$$

$$V_2 = -jB_{zo}A\frac{\omega}{2}\theta_o^2 \tag{6b}$$

In (5) the approximation is valid provided $|\theta_o| \ll 1$. V_1 and V_2 are induced emf phasors corresponding to frequencies ω and 2ω, respectively. Note that V_1 is generally dominant since $|\theta_o| \ll 1$. Consequently, the x component of the earth's magnetic field produces the most significant ac current in the enclosure at the same frequency as the vibration. The above expression for V_1 will be used in the next section to determine the current distribution in the enclosure.

3. CIRCUIT ANALYSIS

The vibrating enclosure can be viewed as a single-turn loop with a circuit representation as a lossy inductor in the frequency range of interest (50 - 100 Hz). Fig. 4 illustrates a simple circuit model showing the interaction of the vibrating enclosure and the enclosed antenna. Note that the enclosure and the loop antenna are inductively coupled through the mutual inductance M. The circuit equations for Fig. 4 are as follows:

$$v(t) = R_i i_1 + (L_i + L_e)\frac{di_1}{dt} + M\frac{di_2}{dt} \tag{7a}$$

$$0 = M\frac{di_1}{dt} + (R_a + R_L)i_2 + L_a\frac{di_2}{dt} \tag{7b}$$

where R_i and L_i are the internal resistance and inductance of the enclosure, respectively, while L_e is the external inductance of the enclosure. R_a and L_a represent the resistance and inductance, respectively, of the loop antenna while R_L is the load resistance. The emf voltage induced in the

enclosure is given by $v(t)$ while $i_1(t)$ is the total current flowing circumferentially in the enclosure. The current $i_2(t)$ flows through the loop antenna. The dot convention in Fig. 4 refers to the calculation of the mutual inductance between the enclosure and loop antenna [1].

Next we will consider the steady-state frequency response of the circuit in Fig. 4 given an excitation frequency of ω rad/s. If the currents and voltage in Fig. 4 are replaced by phasor quantities, the circuit equations (7) become

$$V = [R_i + j\omega (L_i + L_e)] I_1 + j\omega M I_2 \tag{8a}$$

$$0 = j\omega M I_1 + (R_a + R_L + j\omega L_a) I_2 \tag{8b}$$

The solution of (8) for the phasor current I_1 is

$$I_1 = V \frac{R_a + R_L + j\omega L_a}{\omega^2 M^2 + [R_i + j\omega(L_i + L_e)] [R_a + R_L + j\omega L_a]} . \tag{9}$$

Given a steady-state sinusoidal emf voltage V, the total phasor current I_1 flowing circumferentially in the enclosure is given in (9). In this analysis the current induced in the enclosure is approximated by a uniform solenoidal current sheet with any end effects ignored. The end effects can be safely ignored provided the length of the enclosure is much greater than the maximum cross-sectional dimension.

To simplify the determination of the circuit parameters of the enclosure, consider the geometrical approximation of the actual enclosure by a cylindrical tube of length L, inner radius b, and thickness t as shown in Fig. 5. The radius b is determined by equating the inside cross-sectional areas of the enclosure and the tubular model, yielding

$$b = \sqrt{\frac{H'W'}{2\pi}} \tag{10}$$

where H' and W' are the inside height and width of the enclosure, respectively. From the enclosure dimensions in Fig. 1, we find that $H' = 13.7$ in. and $W' = 22.6$ in. Therefore, (10) yields b = 7.03 in. The axis of the loop antenna is assumed to be coincident with the axis of the tubular enclosure in Fig. 5.

3.1 CURRENT DISTRIBUTION

The current density in the tube is given approximately in cylindrical coordinates by [2]

4

$$\mathbf{J} = \mathbf{a}_\varphi \, J_o \, e^{-(1+j)(\rho-b)/\delta}, \quad b \le \rho \le b + t \tag{11}$$

where δ, the skin depth in aluminum, is

$$\delta = \frac{1}{\sqrt{\pi f \mu_o \sigma}} \tag{12}$$

In (11), $\mathbf{a}_\varphi$ is the unit vector in the azimuth direction, ρ is the radial coordinate, and J_o is the current density along the inner surface of the tube. In (12), f is the vibration frequency of the enclosure and μ_o is the permeability of free space. Note that the following approximations have been made in (11):

(a) The current density is the same as that induced in a plane conductor. This is valid for the tubular enclosure provided $b/\delta > 7$ [2].

(b) The current distribution is independent of φ. This is valid since $2\pi b \ll \lambda_o$, where λ_o is the wavelength in free space.

(c) $\mathbf{J}$ is independent of z as end effects have been ignored. This is valid since $L/b \gg 1$.

The total current flowing in the enclosure is given by

$$I_1 = \iint \mathbf{J} \cdot d\mathbf{A} = J_o \int_0^L \int_b^{b+t} e^{-(1+j)(\rho-b)/\delta} \, d\rho \, dz$$

$$= J_o L \frac{\delta}{(1+j)} \left[1 - e^{-(1+j)t/\delta} \right] \tag{13}$$

If $t > 4\delta$, (13) reduces to

$$I_1 \cong J_o L \frac{\delta}{(1+j)} \tag{14}$$

From (11) and (14), the current density $\mathbf{J}$ can be written in terms of the total current I_1 as

$$\mathbf{J} = \mathbf{a}_\varphi \frac{I_1}{L} \frac{(1+j)}{\delta} e^{-(1+j)(\rho-b)/\delta}, \quad b \le \rho \le b + t \tag{15}$$

To simplify the analysis, the current distribution may be approximated as a solenoidal current sheet and given by

$$\mathbf{J} = \mathbf{a}_\varphi \frac{I_1}{L} \delta(\rho - b_{eff}) \tag{16}$$

where δ is the Dirac delta function and b_{eff} is the effective radius defined by

$$b_{eff} = \frac{\int_b^{b+t} \rho \, e^{-(\rho - b)/\delta} \, d\rho}{\int_b^{b+t} e^{-(\rho - b)/\delta} \, d\rho} = \frac{-t\delta \, e^{-t/\delta} + (\delta + b)\delta \left(1 - e^{-t/\delta}\right)}{\delta \left(1 - e^{-t/\delta}\right)} \qquad (17)$$

If $t > 4\delta$, (17) reduces to

$$b_{eff} \cong b + \delta \qquad (18)$$

Thus the induced current in the tubular enclosure is approximated by a circumferentially directed surface current I_1/L that is uniformly distributed over its length with an effective radius of $b + \delta$. This approximation will simplify the determination of the external inductance L_e of the enclosure and the mutual inductance M between the loop antenna and the enclosure.

3.2 DETERMINATION OF CIRCUIT PARAMETERS

The internal resistance R_i and inductance L_i of the enclosure can be determined from the expression for the internal impedance of a flat plane conductor of length $2\pi b$ and are given by [2]

$$R_i = \omega L_i = \frac{2\pi b}{\sigma \delta L} \qquad (19)$$

This formula is valid provided $L \gg b$ and $t > 3\delta$.

The external inductance L_e of the tube is determined by approximating it as a solenoidal current sheet of radius b_{eff} as expressed by (16). In this case the inductance is given by [3]

$$L_e = \frac{\mu_o \pi b_{eff}^2 K}{L} \qquad (20)$$

where K is Nagaoka's constant, a function of the radius and length of the sheet. K is given by a complicated relation involving elliptic integrals and is plotted in [4]. The expression (20) assumes that the current sheet encloses a region that is filled with air (permeability $= \mu_o$). However, since a loop antenna with a magnetic core of permeability μ lies within the enclosure, the effect of this medium must be accounted for in the determination of L_e. The magnetic core may be accounted for by replacing μ_o in (20) by an effective permeability μ_{eff}. Thus (20) is replaced by

$$L_e = \frac{\mu_{eff} \pi b_{eff}^2 K}{L} \tag{21}$$

where

$$\mu_{eff} = \mu_o \left[1 + \frac{a^2}{b_{eff}^2} (\mu_r - 1) \right] . \tag{22}$$

In (22), a is the radius and μ_r is the relative permeability of the core.

The mutual inductance M between the loop antenna and the enclosure can be obtained by considering the coupling between two concentric, coaxial, solenoidal current sheets as described in Fig. 6. If the loop antenna is approximated as a single layer solenoid, the mutual inductance is approximately given by [5]

$$M = 1.57 \, \mu_{eff} \frac{a_2^2 \, N_1 \, N_2}{\chi} \left[1 + \frac{a_1^2 a_2^2}{8\chi^4} \left(3 - \frac{L_2^2}{a_2^2} \right) \right] \tag{23}$$

where

$$\chi = \sqrt{a_1^2 + \frac{L_1^2}{4}} \tag{24}$$

In (23), L_1 is the axial length, a_1 is the radius, and N_1 is the total number of turns on the outer solenoid (enclosure) while L_2, a_2, and N_2 are the corresponding quantities for the inner solenoid (loop antenna). The effect of the magnetic core of the loop antenna is accounted for through the effective permeability μ_{eff} as defined in (22). Expression (23) is an extension of a formula derived for the case of an air core. Additional formulas similar to (23) also appear in the literature [6 - 7] for the case of an air core. In the application of (23) to this problem, a_1 is the effective radius b_{eff} of the enclosure as defined in (18) while a_2 is approximated as the average of the inner and outer radii of the loop antenna.

4. DETERMINATION OF THE AXIAL MAGNETIC FIELD

Consider a current distribution **J** in an infinite homogeneous medium as described in Fig. 7. From the Biot-Savart law [8], the total magnetic field at a point **r** is given by

$$H(r) = \frac{1}{4\pi} \iiint \frac{J(r') \times (r - r')}{|r - r'|^3} \, dv' \tag{25}$$

where the primes denote integration variables while r and r' denote position vectors corresponding to the observation and source points, respectively. The geometry for application of the Biot-Savart law is given in Fig. 8. The application of the Biot-Savart law (25) for the uniform solenoidal current sheet given in (16) yields the following surface integral:

$$H(r) = \frac{I_1}{4\pi L} \iint \frac{a'_\varphi \times (r - r')}{|r - r'|^3} \, dA' \tag{26}$$

where the integration is over the current sheet of length L and radius b_{eff}. The axial component of magnetic field along the axis of the tube at $(0,0,z)$ is determined through evaluation of (26) in cylindrical coordinates, yielding

$$H_z(0,0,z) = \frac{I_1}{2L} b_{eff}^2 \int_0^L \frac{1}{\left[b_{eff}^2 + (z - z')^2 \right]^{3/2}} \, dz' \tag{27}$$

From [9], No. 165,

$$\int \frac{dx}{(x^2 + \alpha^2)^{3/2}} = \frac{x}{\alpha^2 \sqrt{x^2 + \alpha^2}} \tag{28}$$

where α is a constant. The application of (28) to (27) yields

$$H_z(0,0,z) = \frac{I_1}{2L} \left[\frac{z}{\sqrt{z^2 + b_{eff}^2}} + \frac{L - z}{\sqrt{(L - z)^2 + b_{eff}^2}} \right] \tag{29}$$

The magnetic field at the center of the tube $(0,0,L/2)$ is

$$H_z(0,0,L/2) = \frac{I_1}{\sqrt{L^2 + 4b_{eff}^2}} \tag{30}$$

Note that the effect of the magnetic core has been ignored in (25) - (27). As a first approximation, the magnetic field at the center of the tube will not change appreciably from (30) when the magnetic

core is present since H_z is continuous across the longitudinal surface of the core.

5. NUMERICAL RESULTS

In this section, we will determine the axial magnetic field produced by the enclosure at a vibration frequency of 100 Hz. In the vicinity of the measurement site at Fishers Island, NY, the earth's magnetic flux density is $B = 0.5$ Gauss $= 5 \times 10^{-5}$ Wb/m^2 at an angle of approximately 70° with respect to the axis of the enclosure as shown in Fig. 9. It is assumed that the earth's magnetic induction vector B lies entirely in the plane of vibration of the enclosure. Consequently,

$$B_{xo} = B_o \cos 70° = 1.71 \times 10^{-5} \text{ Wb/m}^2.$$

This assumption will result in a maximum ac magnetic field produced by the enclosure. From (6a), the induced emf voltage (per radian of peak vibration θ_o) in the enclosure is

$$V = V_1 = B_{xo}\pi b^2 \omega = 1.08 \times 10^{-3} \text{ Volts/rad.}$$

Note that this voltage is at 100 Hz.

At 100 Hz, the skin depth in aluminum is (from (12)) $\delta = 0.323$ in. Since the thickness ($t = 4$ in.) of the aluminum is greater than 4 skin depths ($t/\delta = 12.4$), the approximation (18) is valid, yielding an effective enclosure radius $b_{eff} = b + \delta = 7.35$ in. The conditions assumed in section 3.1 are satisfied ($b/\delta = 21.8 > 7$, $2\pi b/\lambda_o = 3.74 \times 10^{-7} \ll 1$, $L/b = 10.8 \gg 1$, $t/\delta = 12.4 > 4$), thereby validating the approximation of the current density given by (15).

The loop antenna has a magnetic core with effective permeability $\mu_r = 230$ and radius $a = 1$ in. Therefore, the effective permeability of the medium interior to the enclosure is $\mu_{eff} \cong 5.24 \mu_o$ as obtained from (22). With $L = 76$ in. and $b_{eff} = 7.35$ in., the length to effective diameter ratio of the enclosure is $L/2b_{eff} = 5.17$. Consequently, from [4], Nagaoka's constant for the enclosure is $K \cong 0.92$, resulting in an external inductance $L_e \cong 0.344 \mu$H as obtained from (21). From (19), the internal resistance and reactance of the enclosure are $R_i = \omega L_i = 1.88 \mu\Omega$. Note that the external reactance ωL_e ($= 216 \mu\Omega$) is much greater than the internal resistance and reactance.

In the determination of the mutual inductance M between the enclosure and the loop antenna, the parameters of the enclosure are $N_1 = 1$ turn, $a_1 = b_{eff} = 7.35$ in., and $L_1 = L = 76$ in. The parameters for the loop antenna are $N_2 = 30,800$ turns, $a_2 = 1.30$ in., and $L_2 = 24.25$ in. Note that a_2 is the average of the inner and outer radii, 1.125 in. and 1.475 in., respectively, of the loop antenna. The substitution of these parameters into (23) yields $M = 353 \mu$H.

The circuit parameters of the loop antenna as shown in Fig. 4 are $R_a = 845 \Omega$, $L_a = 592$ H, and $R_L = 15$ MΩ. These values were determined experimentally. With the above circuit parameters, we obtain the following impedances at 100 Hz: $\omega M = 2.22$ mΩ, $|R_i + j\omega(L_i + L_e)| \cong \omega L_e = 0.216$ mΩ, $|R_a + R_L + j\omega L_a| \cong R_L = 15$ MΩ. Therefore,

$$(\omega M)^2 \ll |R_i + j\omega(L_i + L_e)| \; |R_a + R_L + j\omega L_a|$$

Thus (9) reduces to

$$I_1 \cong \frac{V}{R_i + j\omega(L_i + L_e)} \cong \frac{V}{j\omega L_e} \qquad (31)$$

The above expression indicates that the enclosure is effectively decoupled from the loop antenna. From (31), the magnitude of the total current per radian of peak vibration θ_o in the enclosure is $|I_1| = 4.95$ A/rad. Therefore, from (30), the magnetic field strength per radian of peak vibration θ_o at the center of the loop antenna is $|H_z(0,0,L/2)| = 2.52$ A/m·rad. From experiment, the peak vibration angle is $\theta_o = 1.40 \times 10^{-8}$ rad. Thus the magnetic field strength is

$$|H_z(0,0,L/2)| = 3.53 \times 10^{-8} \text{ A/m} = -149 \text{ dBA/m}.$$

In comparison, the field strength measured by the loop antenna was -140 dBA/m, 9 dBA/m higher than the computed result. The difference between the computed and measured results may be attributed to the various approximations made in the model. In spite of this difference, the analysis shows that the vibrating enclosure produces a significant ac magnetic field at 100 Hz.

6. SUMMARY AND CONCLUSIONS

A steady-state time-harmonic analysis has been applied in the determination of the time-varying axial magnetic field produced by a vibrating enclosure in the presence of the earth's magnetic field. The analysis was simplified through the application of circuit theory and the representation of the enclosure as a lossy inductor. Inductive coupling between the enclosure and a stationary loop antenna placed coaxially within it was considered but found to be insignificant.

The computed magnetic field strength at the center of the enclosure was found to be 9 dBA/m below the field measured by the loop antenna at 100 Hz. The difference between the computed and measured results may stem from various approximations made in the model. Some key simplifications made in the model are as follows:

(a) The enclosure was approximated as a tube.

(b) The loop antenna axis was placed coincident with the axis of the enclosure.

(c) The perturbation of the earth's dc magnetic field in the vicinity of the enclosure due to the presence of the magnetic core was ignored.

(d) The perturbation of the ac magnetic field of the vibrating enclosure due to the presence of the magnetic core was neglected.

(e) End effects associated with both the enclosure and magnetic core were ignored.

The inner radius of the tubular enclosure was determined by equating its inside cross-sectional

area with that of the actual enclosure. This was done since the enclosure was modeled as an inductor, making it important to equate the magnetic fluxes passing through each enclosure.

Nonetheless, this analysis shows that the vibrating enclosure produces a significant magnetic field. It has been assumed that the earth's magnetic field lies in the plane of vibration of the enclosure. Thus the computed magnetic field is a maximum.

An alternative analysis can be performed by solving Maxwell's equations in the rest frame of the moving medium (enclosure) through the use of the Maxwell-Lorentz Transformation [10]. In this method, the induced current distribution in the enclosure and resulting magnetic field are determined in the rest frame of the enclosure followed by a transformation of the magnetic field to the rest frame of the earth. This approach was considered but appeared quite unwieldy.

7. REFERENCES

1. W. H. Hayt, Jr. and J. E. Kemmerly, *Engineering Circuit Analysis*, Third Edition, pp. 486 - 495, New York, NY, 1975.

2. S. Ramo, J. R. Whinnery, and T. Van Duzer, *Fields and Waves in Communication Electronics*, Ch. 5, J. Wiley and Sons, New York, NY, 1965.

3. S. Shenfeld, "Prediction of Coupling, Shielding, and Grounds for Low-Frequency Fields", pp. 93 - 97, NUSC Report No. 4051, Naval Underwater Systems Center, New London, CT, 2 April 1971.

4. G. S. Smith, "Loop Antennas", Ch. 5 in *Antenna Engineering Handbook*, Second Edition, edited by R. C. Johnson and H. Jasik, McGraw-Hill, New York, NY, 1984.

5. F. E. Terman, *Radio Engineers' Handbook*, pp. 71 - 72, McGraw-Hill, New York, NY, 1943.

6. F. W. Grover, *Inductance Calculations: Working Formulas and Tables*, Dover Publications, New York, NY, 1962.

7. C. Snow, "Formulas for Computing Capacitance and Inductance", NBS Circular 544, National Bureau of Standards, Washington, DC, 10 September 1954.

8. J. A. Stratton, *Electromagnetic Theory*, pp. 232 - 233, McGraw-Hill, New York, NY, 1941.

9. W. H. Beyer (ed.), *CRC Standard Mathematical Tables*, 28th Edition, CRC Press, Boca Raton, FL, 1987.

10. W. F. Hughes and F. J. Young, *The Electromagnetodynamics of Fluids*, Ch. 2, J. Wiley and Sons, New York, NY, 1966.

(a) 4-in. Thick Welded Aluminum Enclosure
(b) Rigid Antenna Carriage
(c) Loop Antenna
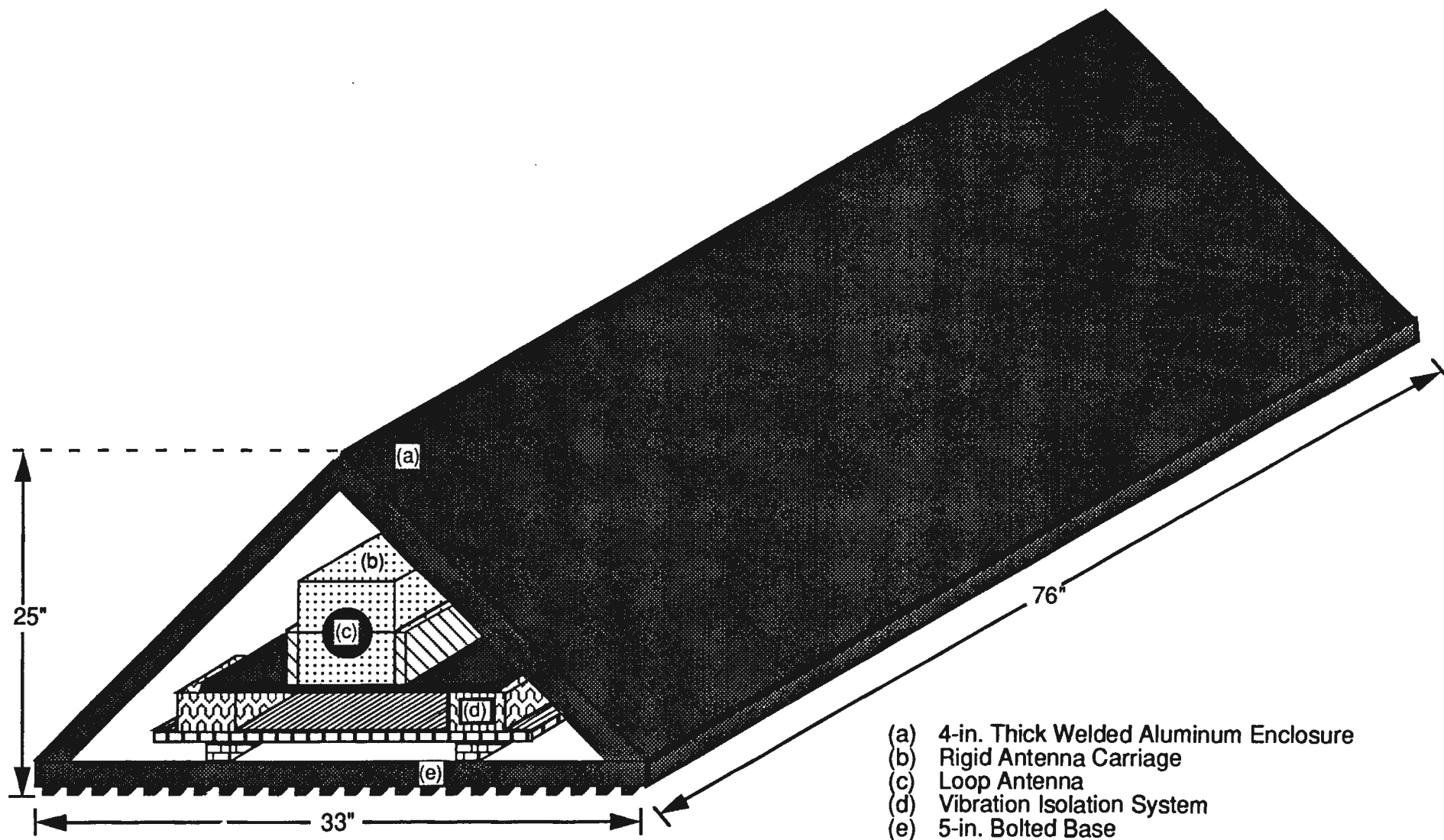(d) Vibration Isolation System
(e) 5-in. Bolted Base

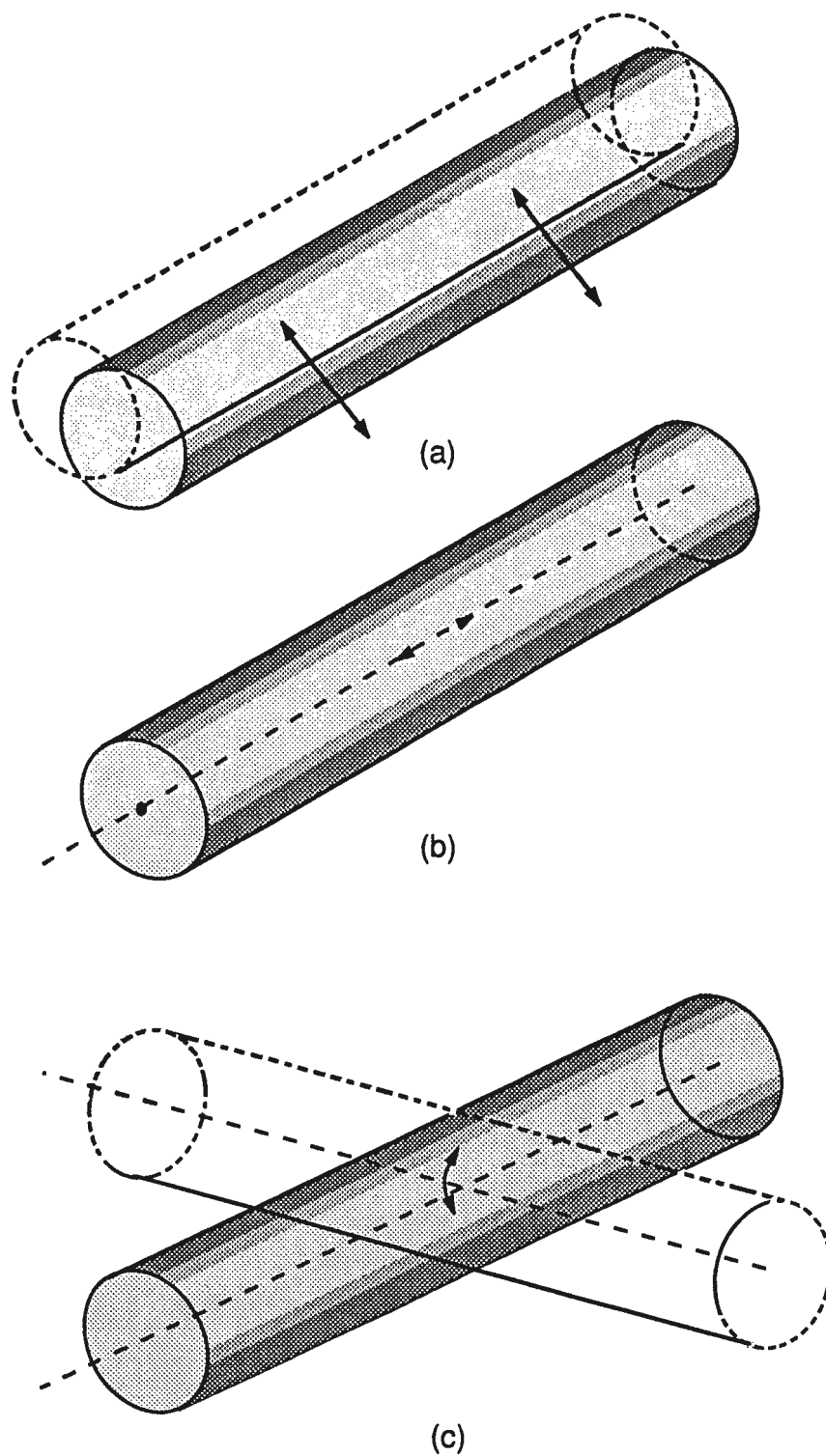Figure 1. Aluminum enclosure and loop antenna system.

Figure 2. Types of vibratory motion.
(a) Translational motion in the radial direction.
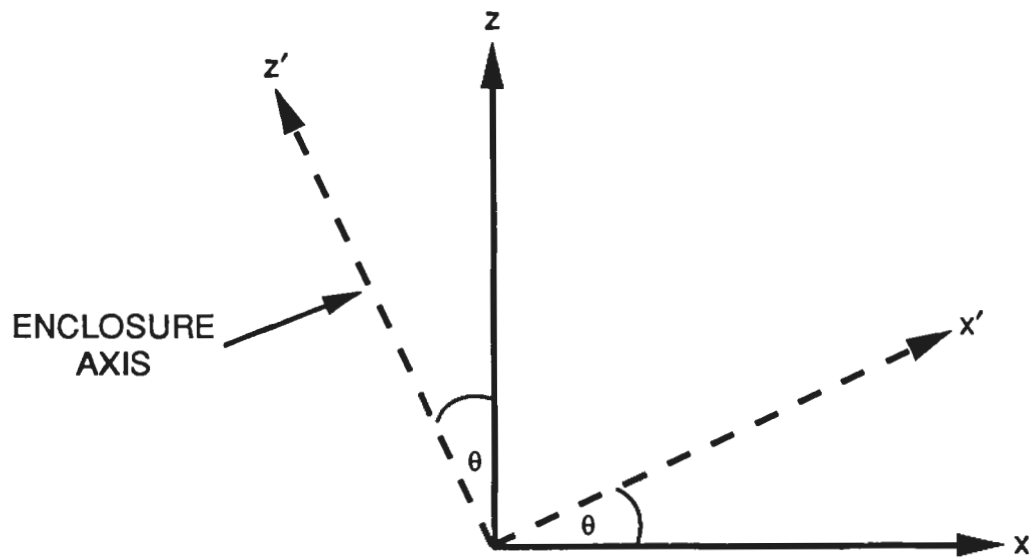(b) Translational motion in the axial direction.
(c) Rotational motion.

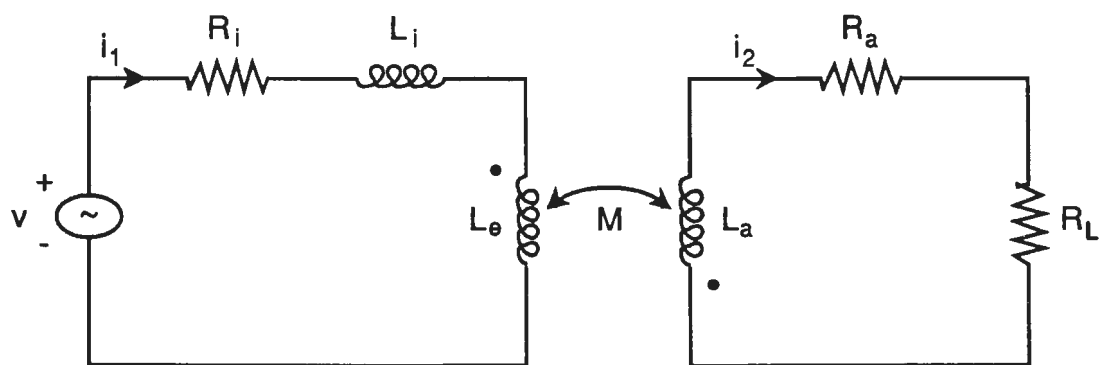Figure 3. Coordinate system transformation.

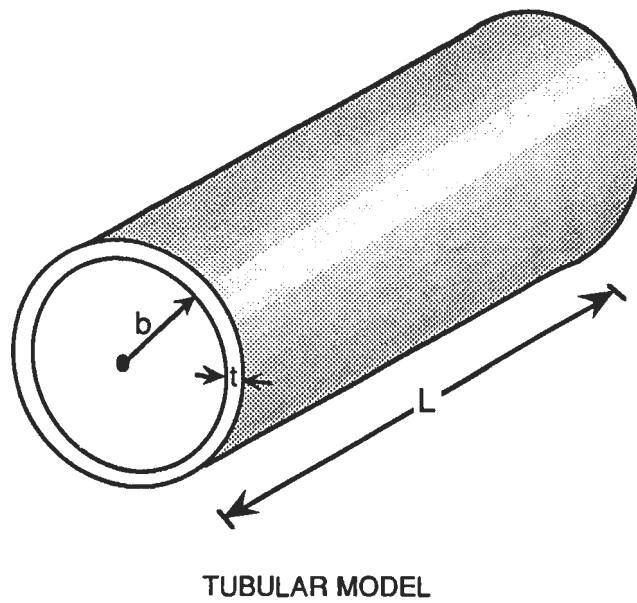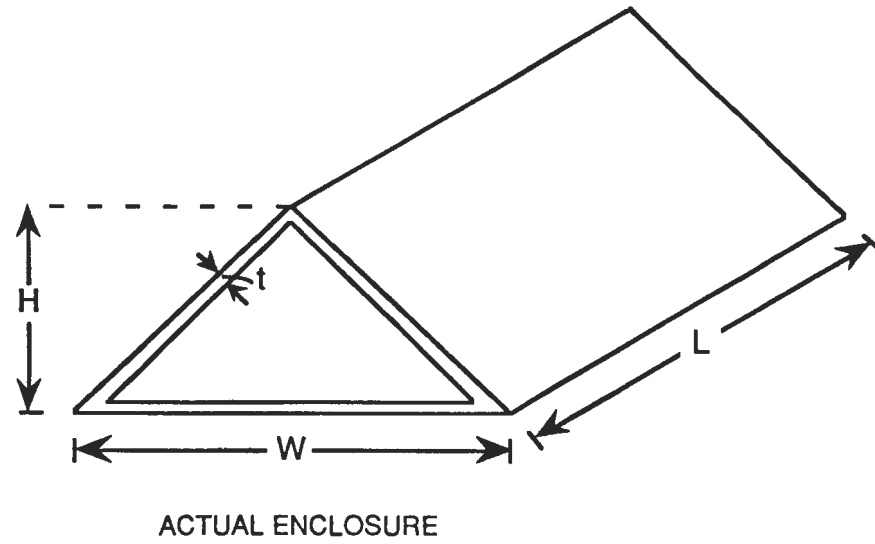Figure 4. Equivalent circuit of the vibrating enclosure and loop antenna.

ACTUAL ENCLOSURE

TUBULAR MODEL

Figure 5. Approximation of the actual enclosure by a tube.
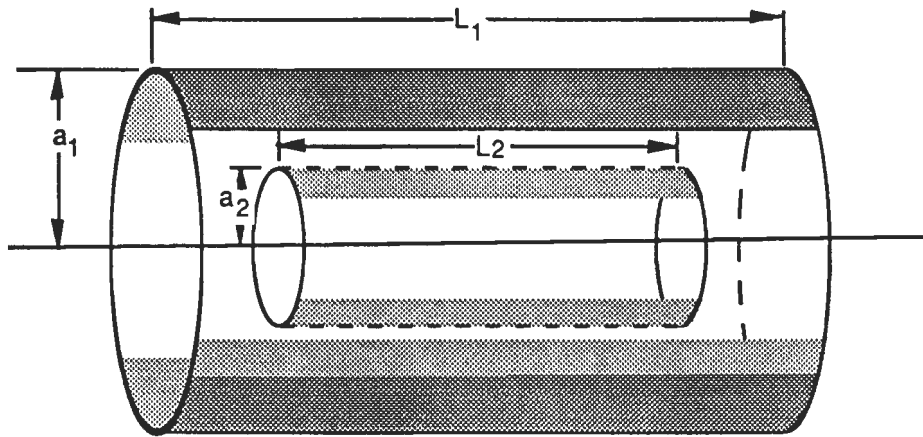
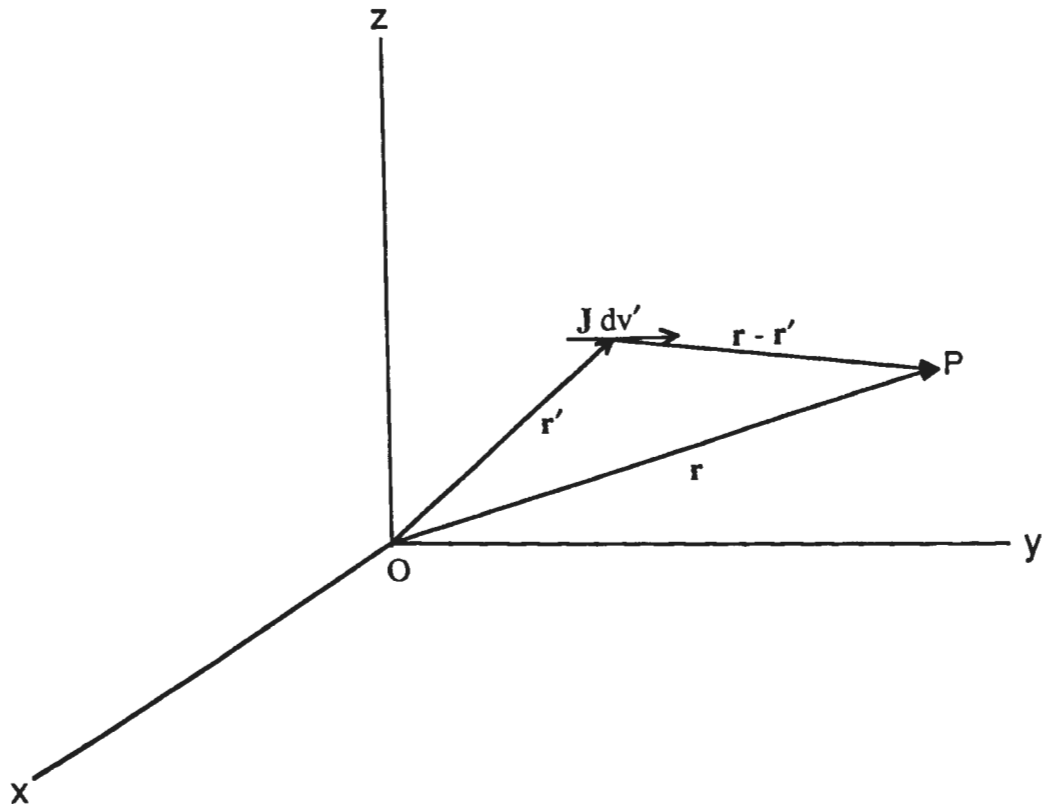Figure 6. Geometry for two concentric, coaxial, solenoidal current sheets.

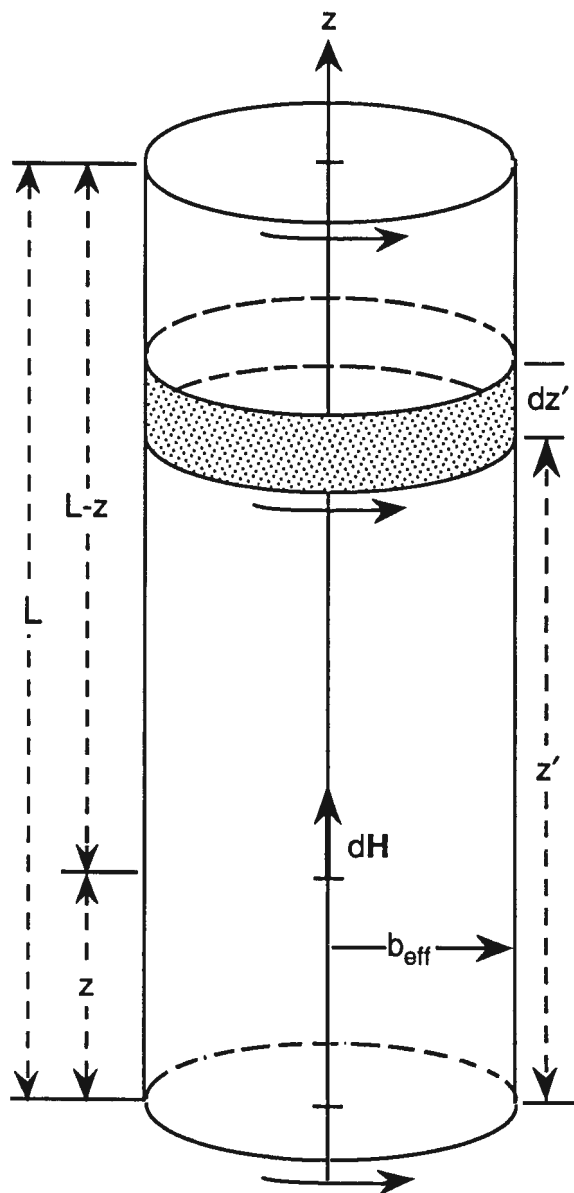Figure 7. Geometry for deducing the magnetic field at P due to a current element **J** dv'.

Figure 8. Geometry for determination of the axial magnetic field along the axis of a solenoidal current sheet.

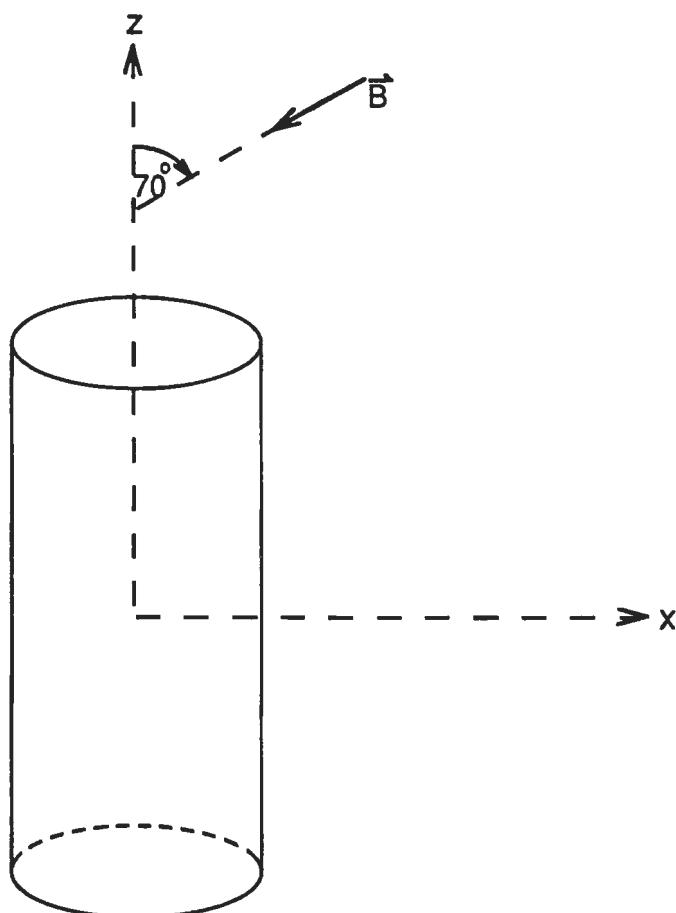Figure 9. Earth's dc magnetic field with the tubular enclosure at rest.

Code 10
Code 102   Dr. K. Lima
Code 103   Dr. E. Sullivan
Code 34
Code 34A
Code 341
Code 341   C. Fessenden
Code 3411
Code 3411   E. Cheng
Code 3411   J. Katan
Code 3411   W. Kraimer
Code 3411   E. Wolkoff
Code 3412   R. Ingram (6)
Code 3413
Code 3413   G. Alvandian
Code 3413   Dr. J. Casey (7)
Code 3413   J. Comiskey
Code 3413   W. Craig
Code 3413   Dr. D. Fessenden
Code 3413   E. Gerhard
Code 3413   P. Gilles
Code 3413   K. Hafner
Code 3413   Dr. C. Kim
Code 3413   P. Mileski
Code 3413   D. Nordstrom
Code 3413   Dr. B. Panoutsopoulos
Code 3413   B. Pease
Code 3413   D. Portofee
Code 3413   A. Ramirez
Code 3413   D. Rivera
Code 3413   S. Safford
Code 3413   D. Saleem
Code 3413   C. Spellman
Code 342
Code 3421
Code 3422
Code 3422   Dr. T. Anderson
Code 343
Code 3431
Code 3431   L. Dalsass
Code 3431   D. Gumkowski
Code 3491
Code 3496
Code 412   Dr. R. Kasper
Code 412   A. Bruno
Code 4221   A. Jagaczewski
Code 4221   R. Lafreniere
Code 0211   A. Mastan
Code 0261   Library (New London) (3)
Code 0262   Library (Newport) (3)

External: 0
Internal: <u>65</u>
Total: 65